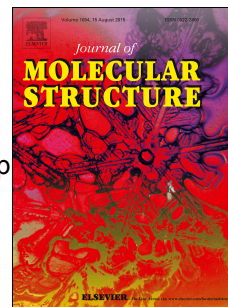


# Journal Pre-proof

Acceptor- $\pi$ -Acceptor-Acceptor/Donor systems containing dicyanovinyl acceptor group with substituted 1,2,3-triazole motif – synthesis, photophysical and theoretical studies

Dawid Zych, Aneta Slodek



PII: S0022-2860(19)31597-2

DOI: <https://doi.org/10.1016/j.molstruc.2019.127488>

Reference: MOLSTR 127488

To appear in: *Journal of Molecular Structure*

Received Date: 12 October 2019

Revised Date: 26 November 2019

Accepted Date: 27 November 2019

Please cite this article as: D. Zych, A. Slodek, Acceptor- $\pi$ -Acceptor-Acceptor/Donor systems containing dicyanovinyl acceptor group with substituted 1,2,3-triazole motif – synthesis, photophysical and theoretical studies, *Journal of Molecular Structure* (2019), doi: <https://doi.org/10.1016/j.molstruc.2019.127488>.

This is a PDF file of an article that has undergone enhancements after acceptance, such as the addition of a cover page and metadata, and formatting for readability, but it is not yet the definitive version of record. This version will undergo additional copyediting, typesetting and review before it is published in its final form, but we are providing this version to give early visibility of the article. Please note that, during the production process, errors may be discovered which could affect the content, and all legal disclaimers that apply to the journal pertain.

© 2019 Published by Elsevier B.V.

# Acceptor- $\pi$ -Acceptor-Acceptor/Donor systems containing dicyanovinyl acceptor group with substituted 1,2,3-triazole motif – synthesis, photophysical and theoretical studies

Dawid Zych<sup>[a]\*</sup> and Aneta Slodek<sup>[b]</sup>

[a] Institut für Silizium-Photovoltaik, Helmholtz-Zentrum Berlin für Materialien und Energie GmbH, Kekuléstraße 5, 12489 Berlin, Germany

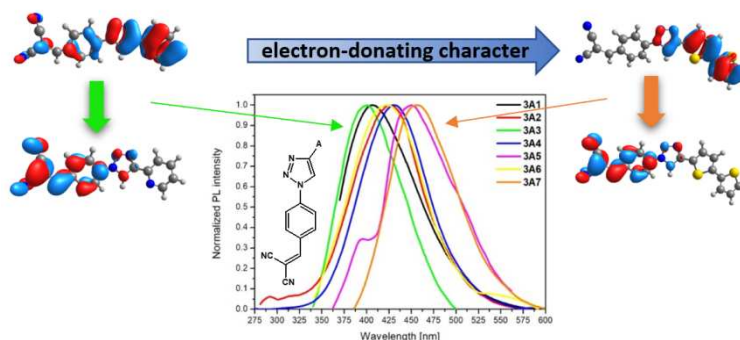
[b] Institute of Chemistry, University of Silesia, Szkolna 9, 40-007 Katowice, Poland

\*Corresponding Author: [dawidzych92@gmail.com](mailto:dawidzych92@gmail.com) (Dr. Dawid Zych)

D. Zych ORCID 0000-0002-7757-7321

A. Slodek ORCID 0000-0003-2600-6518

## Graphical abstract



## Highlights

- Acceptor- $\pi$ -Acceptor-Acceptor/Donor ( $-\text{CH}_2(\text{CN})_2$ )- $\text{C}_6\text{H}_4$ -/triazole/substituent) systems
- Effective synthetic routes for the synthesis of compounds containing dicyanovinyl acceptor group with substituted 1,2,3-triazole motif
- Photophysical investigations supported by quantum-chemical calculations
- Druglikeness analysis based on the physicochemical properties and lipophilicity

## Abstract

An efficient synthetic route (target products obtained with yields 65-85%) for obtaining of malononitrile derivatives containing triazole motif substituted in the way providing the electronic architecture Acceptor- $\pi$ -Acceptor-Acceptor/Donor ( $-\text{CH}_2(\text{CN})_2$ )- $\text{C}_6\text{H}_4$ -/triazole/substituent) is presented. As the substituents phenyl (A1), *p*-pentyloxyphenyl (A2), pyrid-2-yl (A3), 9,9-dimethylfluoren-2-yl (A4), 9-octyl-9*H*-carbazol-3-yl (A5), dibenzo[*b,d*]thiophen-2-

yl (A6) and 2,2'-bithiophenyl-5-yl (A7) were used. The structures of compounds were confirmed by  $^1\text{H}$  and  $^{13}\text{C}$  NMR spectroscopy. The thermal, optical and photophysical properties of obtained target compounds were checked. Understanding of obtained data was supported by quantum-chemical calculations based on DFT methods (time-dependent calculations, NTO analysis, structural parameters). Moreover, the druglikeness analysis was performed based on the commonly known rules.

**Keywords:** Acceptor-Donor system; 1,2,3-triazole motif; dicyanovinyl group; optical and photophysical properties; theoretical studies; druglikeness analysis

## 1. Introduction

Molecules built from electron-donating and electron-accepting groups have become the interest of researcher due to the wide spectrum of possible applications [1–4]. Moreover, the constant development of chemical reactions, including the discovery of Cu(I)-catalyzed Huisgen 1,3-dipolar cycloaddition reaction caused that more and more molecules contain in the structure triazole bridges as versatile linkers [5–10]. When we also add next well-established reaction - Knoevenagel condensation, the broad area of the functionalization appears [11]. Taking into account compounds containing triazole and malononitrile groups, they were reported as materials which can be used as chemosensors [12–14] and chromophores [15]. In the case of chemosensors, all described in literature examples are dedicated to the sensing of cyanide anion [8–10]. Introduction of malononitrile moiety to the structure of molecules can also result in obtaining of materials which can be used as chemosensors for thiocyanate [16] and sulfite anion [17].

Peter D. Jarowski et al. presented 1,2,3-triazoles as conjugative  $\pi$ -linkers in push-pull chromophores and the influence of isomeric charge-transfer between the 1,2,3-triazole motif and dicyanovinyl group on the optical properties of target systems [15]. They reported that the change of the maxima absorption is about 50 nm (experimentally) and 100 nm (theoretically calculated) depending on the position of the substituent.

Compounds structurally similar to molecules, which are a subject of our study, containing malononitrile group connected to phenyl ring which is substituted at the *para* position by (hetero)aryl group are in the great interest of scientist during the last years. That compounds contain one or two malononitrile moieties. Molecules with two malononitrile groups were reported by G. Marianetti et al. with application as solar collectors based on 2,5-

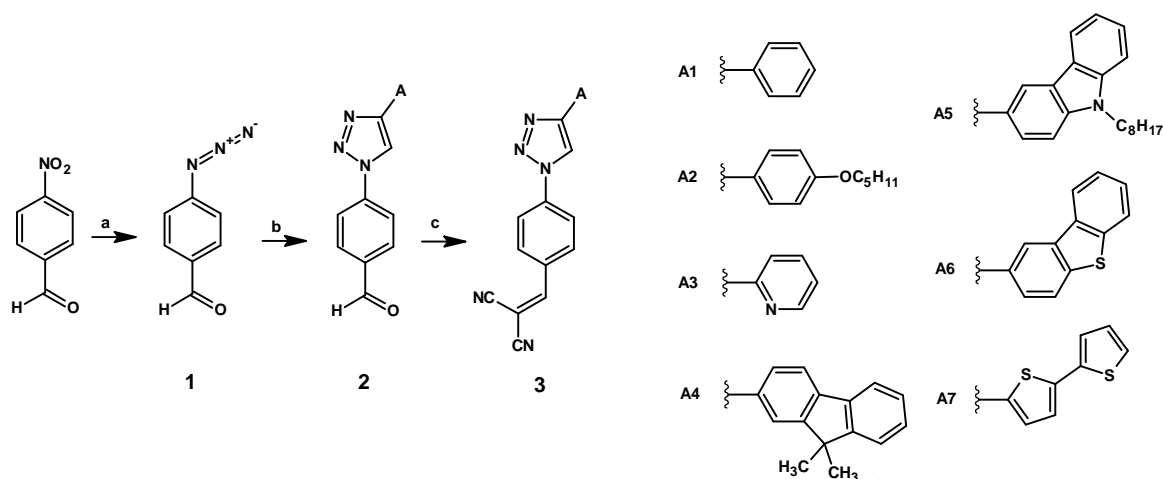
diarylimidazoles [18], R. Dominguez and co-workers presented tetraaryl-1,4-dihydropyrrolo[3,2-*b*]pyrrole dedicated to organic solar cells [19] and also by P. Wen et al. with carbazole moiety as a lead structure which exhibits remarkable solvatochromism effect [1]. In the case of monosubstituted by dicyanovinyl group, the work of Z. Li et al. can be found where authors described multi-modulated photochromic behaviour of a D-A type dithienylethene [20], and results of Y. J. Chang and co-workers with carbazole-based small molecules for vacuum-deposited organic photovoltaic devices with promising parameters [21].

We have recently reported the synthesis and comprehensive characterization of the derivatives of 4'-(1,2,3-triazol-4-yl)phenyl-2,2':6',2''-terpyridine with various (hetero)aryl substituents, where the first approach to their synthesis started with the substitution of the nitro group in 4-nitrobenzaldehyde by the azide anion which was subjected to a 1,3-dipolar cycloaddition reaction with ethynyl derivatives of (hetero)aryls followed by aldol condensation reaction what resulted in target products with low yields [22]. Here we decided to present the other possibility of using of 4-(4-substituted-1*H*-1,2,3-triazol-1-yl)benzaldehyde, this time in the synthesis of malononitrile derivatives (with architecture Acceptor- $\pi$ -Acceptor-Acceptor/Donor (-CH<sub>2</sub>(CN)<sub>2</sub>-C<sub>6</sub>H<sub>4</sub>-triazole/substituent) with the studies of their optical and photophysical properties supported by quantum-chemical calculations based on DFT methods. Moreover, the druglikeness analysis was performed based on the published in literature Lipiński, Ghose, Veber, Egan and Muegge rules.

## 2. Results and discussion

### 2.1. Synthesis and structural characterization

The structures of target compounds **3A1-7** and route for their synthesis are presented in Scheme 1. 4-(4-Substituted-1*H*-1,2,3-triazol-1-yl)benzaldehydes were obtained by using the way which was already reported by us, starting from substitution of nitro group of 4-nitrobenzaldehyde by azide group followed by Cu(I)-catalyzed Huisgen 1,3-dipolar cycloaddition with ethynyl derivatives of (hetero)aryls what resulted in **2A1-7** with satisfactory yields in the range of 60-78% [22]. These intermediates were used in the next step - Knoevenagel condensation with malononitrile by using the heterogeneous phase as an inorganic catalyst - aluminium oxide in dichloromethane solution what resulted in target products **3A1-7** with yields 65-85% [23]. The structures of compounds were confirmed by <sup>1</sup>H and <sup>13</sup>C NMR spectroscopy (Supporting Information S1-S21).



**Scheme 1.** Synthesis of compounds **1**, **2A1-7**, and **3A1-7**. *Reagents and conditions:* a)  $\text{NaN}_3$ , HMPA, room temp., 72 h, 90% yield; b) ethynyl-derivative of A1-7,  $\text{CuSO}_4 \cdot 5\text{H}_2\text{O}$ , sodium ascorbate, pyridine, EtOH,  $\text{H}_2\text{O}$ , room temp., 24 h; c) malononitrile,  $\text{Al}_2\text{O}_3$ , DCM, room temp., 24 h.

## 2.2. Theoretical calculations

To gain the structural parameters and deep insight into optical and photophysical properties, the quantum-chemical calculations based on DFT and TD-DFT methods were conducted. In order to obtain the results which are sublimely correlated with the experimental data, various exchange-correlation functionals were applied: B3LYP [24], CAM-B3LYP [25], wB97XD [26] and M06 [27] with 6-31G\*\* basis set implemented in the Gaussian 09 program [28]. All geometries were optimized in a chloroform solution in the polarisable continuous model (PCM) [29]. Obtained values of the energy gaps confronted with the values of optical energy gaps (the absolute value of the difference between  $E_{g \text{ opt}}$  and the result of calculation  $|\Delta|$ ) are presented in Table 1.

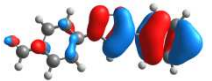
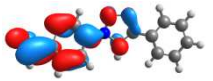
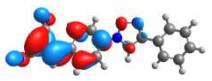
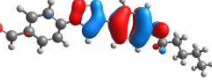
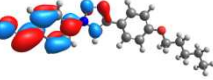
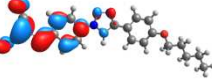
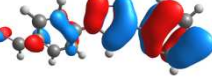
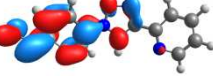
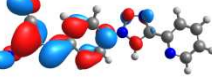
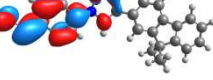
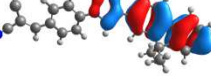
**Table 1.** Energy gaps for **3A1-7** obtained from DFT calculations with various hybrid potentials and 6-31G(d,p) basis set in chloroform compared with optical energy gaps.

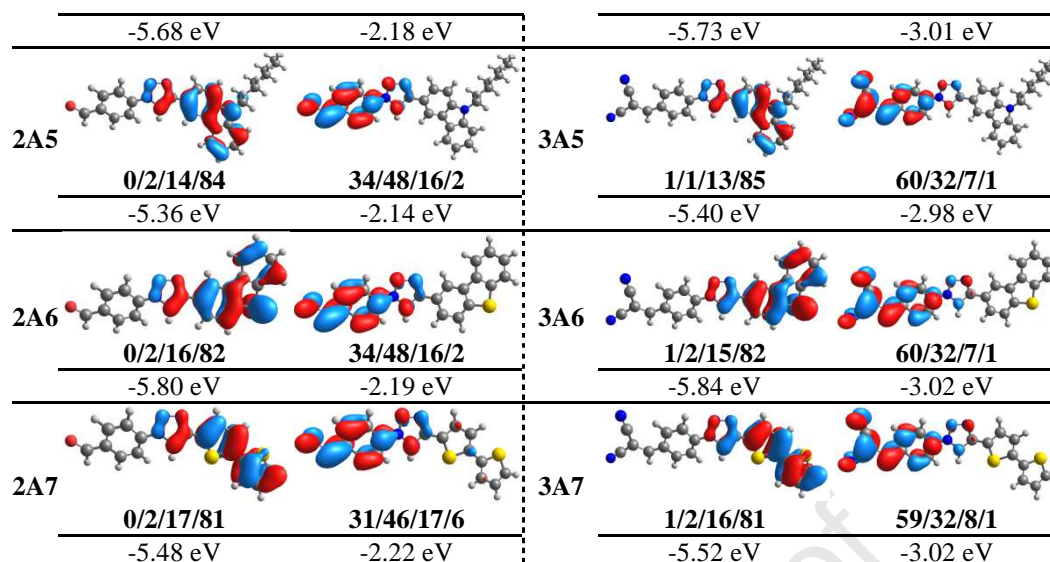
	$E_{g \text{ opt}}$ [eV]	$\Delta E$ [eV]							
		B3LYP	$ \Delta $	CAM-B3LYP	$ \Delta $	wB97XD	$ \Delta $	M06	$ \Delta $
<b>3A1</b>	3.13	3.26	0.13	5.79	2.66	6.92	3.79	3.73	0.60
<b>3A2</b>	2.92	2.78	0.14	5.29	2.37	6.42	3.50	3.25	0.33
<b>3A3</b>	3.19	3.47	0.28	6.02	2.83	7.13	3.94	3.94	0.75
<b>3A4</b>	2.89	2.72	0.17	5.19	2.30	6.31	3.42	3.15	0.26
<b>3A5</b>	2.65	2.42	0.23	4.86	2.21	5.96	3.31	2.90	0.25

<b>3A6</b>	2.93	2.82	0.11	5.30	2.37	6.41	3.48	3.23	0.30
<b>3A7</b>	2.74	2.50	0.24	5.04	2.30	6.16	3.42	2.95	0.21

The values of energy gaps obtained as the result of calculations with B3LYP hybrid potential are the closest to the experimental values and followed the same trend: **3A5**<**3A7**<**3A4**<**3A2**<**3A6**<**3A1**<**3A3**, the energy gap of compound **3A3** containing 2-pyridyl substituents is the highest, whereas **3A5** containing carbazyl unit has the lowest energy difference between frontier orbitals. Moreover, the results obtained with M06 exchange-correlation functional have also physical sense, but the differences are higher in comparison to B3LYP. Also, the trend is changed, the energy gap of **3A6** is lower than of **3A2**. In the case of CAM-B3LYP and wb97XD, the values are much higher, even doubled. Based on the above-presented results, the B3LYP/6-31G(d,p) contours of frontier orbitals with the contribution in their creation of particular parts of molecules **2A1-7** and **3A1-7** (-CHO or -CH<sub>2</sub>(CN)<sub>2</sub>-C<sub>6</sub>H<sub>4</sub>-triazole/substituent) are presented in Table 2. Furthermore, the theoretical investigations were also extended to the substrates of Knoevenagel condensation - aldehydes **2A1-7**, what is also presented in Table 2. All orbitals were computed at an isovalue of 0.03 e/bohr<sup>3</sup>.

**Table 2.** The optimized structures B3LYP/6-31G(d,p) with contours of HOMOs and LUMOs and the contribution of the individual part of molecules (-CHO or -CH<sub>2</sub>(CN)<sub>2</sub>-C<sub>6</sub>H<sub>4</sub>-triazole/substituent) in their creation, and energies of frontier orbitals for **2A1-7** and **3A1-7**.

	HOMO	LUMO		HOMO	LUMO
<b>2A1</b>	 1/8/42/49 -6.22 eV	 34/48/16/2 -2.19 eV	<b>3A1</b>	 4/9/40/47 -6.27 eV	 60/32/7/1 -3.01 eV
<b>2A2</b>	 0/3/25/72 -5.71 eV	 34/49/16/1 -2.16 eV	<b>3A2</b>	 1/3/24/72 -5.77 eV	 60/32/7/1 -2.99 eV
<b>2A3</b>	 2/11/45/42 -6.45 eV	 33/48/17/2 -2.20 eV	<b>3A3</b>	 8/14/41/37 -6.49 eV	 60/32/7/1 -3.02 eV
<b>2A4</b>	 0/3/20/77	 34/48/16/2	<b>3A4</b>	 1/2/19/78	 60/32/7/1



The energies of orbitals H-2, H-1, H, L, L+1, L+2 are depicted in Figure 1. It shows that the exchange of aldehyde group into malononitrile moiety causes the significant reduction of the energy of the lowest unoccupied orbitals (LUMO), what is desirable in the creation of potential materials which can be applied in wide-known organic electronics. It is also worth to emphasize that the energies of the rest of the presented orbitals are similar for the aldehyde and corresponding malononitrile derivative.

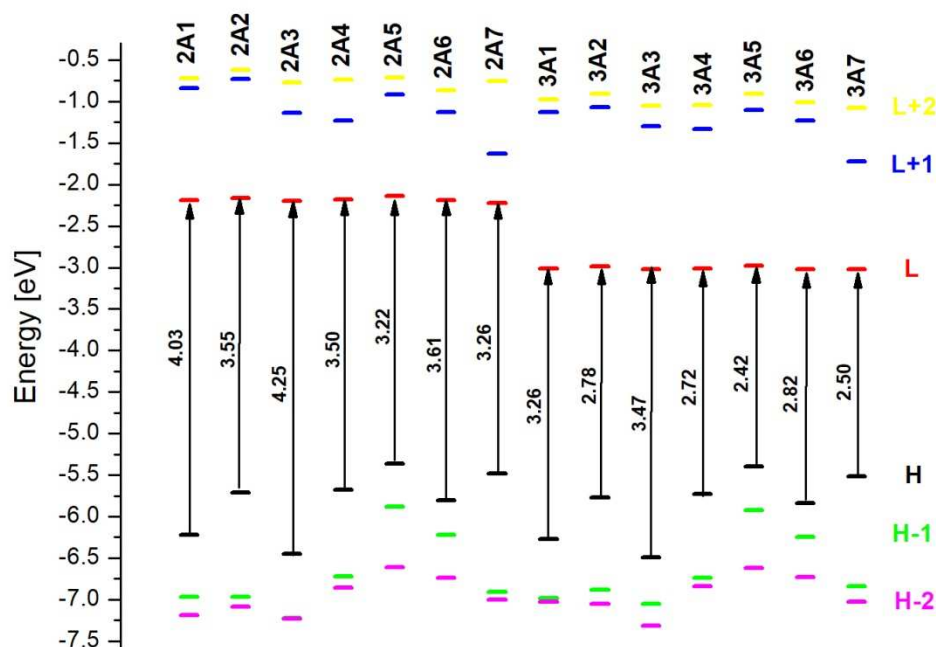


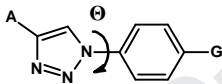
**Figure 1.** Energies of orbitals (B3LYP/6-31G(d,p)): H-2, H-1, H, L, L+1, L+2 for **2A1-7** and **3A1-7**.

Described above dependence is related to the contribution of the individual part of molecules in the creation of orbitals. In the case of HOMOs, the contribution of the

substituent for malononitrile, as well as for aldehyde is the highest for **2A5** (84%) and **3A5** (85%) containing carbazyl group and the lowest for **2A3** (42%) and **3A3** (37%) with 2-pyridyl group. Due to the stronger electron-accepting character of dicyanovinyl group in comparison to the aldehyde group, the significant difference in the creation of the lowest unoccupied orbitals, and therefore, their energies were observed. The contribution of  $-\text{CH}_2(\text{CN})_2$  group in the creation of LUMO for **3A1-7** equals about 60%, whereas the  $-\text{CHO}$  builds HOMO of **2A1-7** in about 31-34%.

What is more, the structural parameters such as the angles between the surface of benzaldehyde or benzylidenemalononitrile and substituted triazole ring were checked. Obtained data are presented in Table 3.

**Table 3.** Calculated (B3LYP/6-31G(d,p)) angles between triazole and phenyl group.



	$\Theta$ [°]		$\Theta$ [°]
<b>2A1</b>	22.48	<b>3A1</b>	18.36
<b>2A2</b>	23.53	<b>3A2</b>	18.11
<b>2A3</b>	22.72	<b>3A3</b>	17.63
<b>2A4</b>	24.27	<b>3A4</b>	20.65
<b>2A5</b>	22.59	<b>3A5</b>	18.79
<b>2A6</b>	24.25	<b>3A6</b>	20.25
<b>2A7</b>	23.54	<b>3A7</b>	19.86

First of all, the significant angles difference between aldehydes and corresponding malononitrile were observed, the values in the case of aldehyde are higher than for corresponding malononitriles. The highest value of the angle in the group of aldehydes was for **2A4** (24.27°), the lowest for **2A1** (22.48°), whereas in the case of malononitriles, the highest for **3A4** (20.65°) and lowest for **3A3** (17.63°). The highest difference between the groups of studied compounds was observed for compounds containing *p*-pentyloxyphenyl substituent **2A2** and **3A2** (5.42°) and the lowest with 9,9-dimethylfluoren-2-yl **2A4** and **3A4** (3.62°).

### 2.3. Optical and photophysical properties

Temperatures of thermal degradation, which correspond to 5 and 10% weight loss during the heating were checked by using thermogravimetric analysis (TGA) under a nitrogen atmosphere up to 900 °C. TGA thermograms and numerical values are presented in Figure 2

and Table 4. The results showed that studied molecules retain varied stability; the most stable is compound **3A3** with decomposition temperature corresponding to 5% weight loss ( $T_{5\%}$ ) at 329 °C. Among examined molecules, **3A3** has the highest char residue at 900 °C. Compound **3A6** exhibits the lowest value of  $T_{5\%}$ . The temperature of 10% weight loss ( $T_{10\%}$ ) for all examined compounds **3A1-7** is higher than 300 °C, the highest for **3A3**, the lowest for **3A7**.

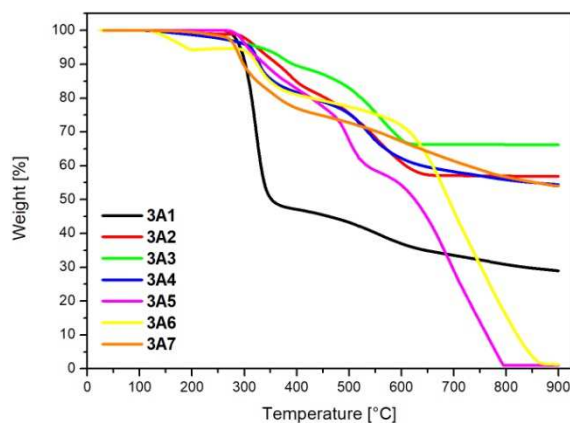


**Figure 2.** TGA curves of **3A1-7**.

**Table 4.** Thermal properties of the synthesized derivatives **3A1-7**.

	$T_{5\%}$ [°C]	$T_{10\%}$ [°C]	Char residue at 900 °C [%]
<b>3A1</b>	292	302	29
<b>3A2</b>	324	364	57
<b>3A3</b>	329	393	66
<b>3A4</b>	312	329	54
<b>3A5</b>	306	339	1
<b>3A6</b>	188	325	1
<b>3A7</b>	283	300	54

The optical properties of **3A1-7** compounds were examined by UV-Vis spectra and photoluminescence (PL) spectroscopy techniques in chloroform solution ( $1 \times 10^{-5}$  M) at ambient temperature. The corresponding optical data and quantum yields are presented in Table 5. The UV-Vis absorption spectra depicted in Figure 3a show several bands in the range of 250-450 nm. The absorption bands in the UV region (250-350 nm) are assigned to the  $\pi-\pi^*$  transitions while the absorption bands appear between 350 and 450 nm which are dominated by HOMO→LUMO transition can be ascribed to the intramolecular charge transfer (ICT) between substituent (A) and -CN groups.

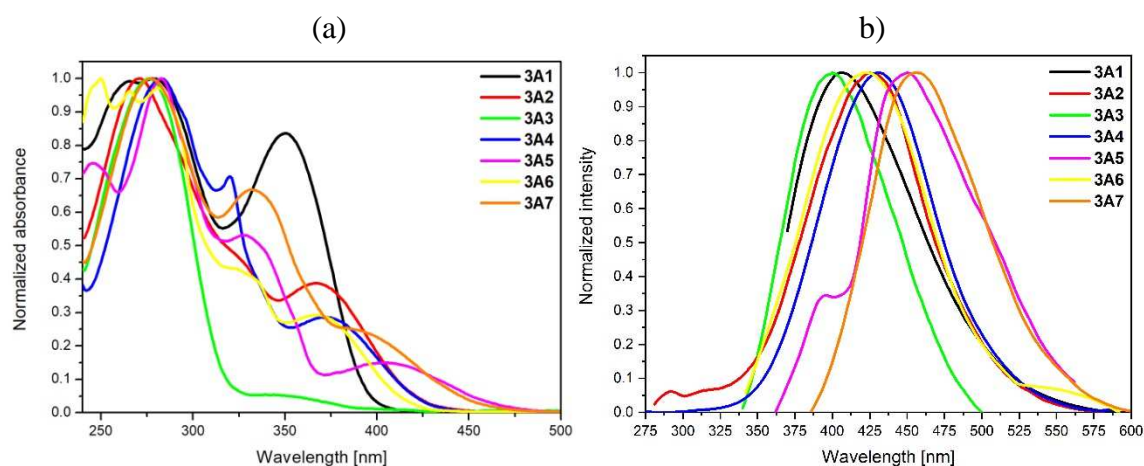


**Figure 3.** Normalized absorption (a) and emission (b) spectra recorded in  $\text{CHCl}_3$  of **3A1-7**.

Compounds **3A1-7** as the simple D-A systems present a strong correlation between the electronic ability of substituents A and their absorption features. Given the electronic nature of substituents A in compounds **3A1-7**, a redshift alike of the  $\pi-\pi^*$  and the ICT bands is observed with increasing the electron-donating ability of substituents A in the following order **3A3**→**3A1**→**3A6**→**3A2**→**3A4**→**3A7**→**3A5**. Compound **3A3** containing pyridine motif with electron-withdrawing character possess less electron releasing nature than bithienyl and carbazyl groups in **3A7**→**3A5** causing the weaker ICT.

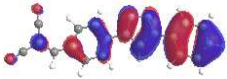
**Table 5.** Photophysical data for **3A1-7** recorded in the chloroform solution.

	$\lambda_{\text{max}}[\text{nm}]$	PL $\lambda_{\text{em}} [\text{nm}]$ / Stokes shift [ $\text{cm}^{-1}$ ]	$\Phi$ [%]
<b>3A1</b>	350	407/3999	15
<b>3A2</b>	367	425/3718	13
<b>3A3</b>	349	401/3716	21
<b>3A4</b>	283, 320, 372	430/3626	52
<b>3A5</b>	245, 283, 329, 404	451/2580	56
<b>3A6</b>	250, 266, 281, 325, 366	423/3682	36
<b>3A7</b>	332, 392	454/3484	62

To more widely assess the effect of the substituent A in compounds **3A1-7** on the absorption properties, TD-DFT calculations in chloroform done with four different hybrid potentials were demonstrated. The results and UV-Vis simulated absorption spectra are depicted in Table S1. TD-DFT calculations performed with CAM-B3LYP, B3LYP, wB97XD, and M06 methods confirmed the absorption spectra dependent on the nature of the substituent A.

Among four different methods, the B3LYP and M06 proved to best reflect the experimental data. CAM-B3LYP and wB97XD hybrid potentials, although they gave a rational description of the high energy absorption bands, did not indicate ICT transitions. The theoretical results will be discussed predominately based on the B3LYP and M06 functionals. The B3LYP and M06 methods gave the depiction of dominate transitions that are slightly shifted by approximately 45 nm relative to experimental data. The red-shifted absorption bands for compounds **3A4**, **3A5**, and **3A7** compared to the other were found, which is in good accord with the experimental results. The presence of strongly electron-donating moieties in **3A4** (fluorene), **3A5** (carbazole), and **3A7** (bithiophene) induces effective charge transfer from substituents A to the cyano groups, confirmed by the distribution of their HOMO orbitals with 78-85% contribution of substituents A and LUMO orbitals mainly populated on the cyano groups with a 60% share. Moreover, the deep insight into the absorption spectra was done by using the natural transition orbitals analysis. The pairs occupied (holes) and unoccupied (electrons) with contribution higher than 20% presenting the nature of absorption spectra (6-31G(d,p)/M06) with the contribution of  $\text{CH}_2(\text{CN})_2$ /- $\text{C}_6\text{H}_4$ -/triazole/substituent is presented for **3A1** in Table 6, NTO analysis for molecules **3A2-7** is presented in Supporting Information as Tables S2-S7. For each state, the respective number of the state, transition energy, and the oscillator strength are listed.

**Table 6.** Natural transition orbitals (NTOs) analysis for **3A1**.

<b>3A1</b>	<b>Hole</b>	<b>Electron</b>
<b>393.14 nm</b> S <sub>1</sub> 3.154 eV (0.560) 98%		
	0.04/0.08/0.34/0.54	0.60/0.33/0.07/0.00
<b>328.23 nm</b> S <sub>2</sub> 3.777 eV (0.758) 97%		
	0.34/0.42/0.12/0.12	0.60/0.33/0.07/0.00
<b>258.07 nm</b> S <sub>6</sub> 4.804 eV (0.107) 93%		
	0.04/0.08/0.34/0.54	0.15/0.18/0.47/0.21
<b>249.59 nm</b> S <sub>7</sub> 4.968 eV (0.212) 88%		
	0.04/0.08/0.34/0.54	0.00/0.37/0.24/0.38

The emission spectra of **3A1-7** are depicted in Figure 3b. Compounds **3A1-7** demonstrate strong blue-greenish photoluminescence (PL) in chloroform solution with the peaks located in the range of 400 - 455 nm. The structural changes associated with the position 4 of the triazole unit of **3A1-7** are quite pronounced and the impact of their electronic capacity on the emission spectrum cannot be ignored. When the bithiophene and carbazole motifs with strong electron-donating character were adopted to the triazole unit in **3A5** and **3A7**, respectively, the fluorescence peaks of presented compounds exhibited redshifts about 50 nm with relative to **3A3**, which possess strong electron-withdrawing pyridine unit. *p*-Pentyloxyphenyl, fluorenyl, and dibenzothiophenyl substituents on triazole unit of **3A2**, **3A4** and **3A6**, respectively, also led to a bathochromic shift similar to compounds **3A5** and **3A7**, but smaller about 20 nm compared with compound **3A3**. Insertion of phenyl unit possessing weak donating ability in the triazole ring in **3A1** resulting in a slightly shifted (6 nm) emission maximum compared to **3A3**. As confirmed by emission spectra, the use of various substituents in the examined compounds **3A1-7** strongly determines photoluminescent behaviour. Concluding from TD-DFT calculations carried out with CAM-B3LYP, B3LYP, wB97XD, and M06; the CAM-B3LYP and wB97XD hybrid potential showed the best fit for the experimental data. The theoretical calculations confirm that the extent of the shift of emission maximum depends on the electron-donating facilities of the substituents in compounds **3A1-7** (Table 7 and S8).

**Table 7.** TD-DFT calculated wavelengths of emission with oscillator strengths for **3A1-7**.

	Exp [nm]		Calculated wavelengths [nm] (oscillator strengths)	$\Delta$ [nm]	Transitions
<b>3A1</b>	407	CAM-B3LYP	390.27 (1.4988)	17	HOMO→LUMO (78%), H-1→LUMO (19%),
		wB97XD	387.96 (1.4928)	19	HOMO→LUMO (73%), H-1→LUMO (23%)
<b>3A2</b>	425	CAM-B3LYP	403.94 (1.3892)	21	HOMO→LUMO (69%), H-1→LUMO (26%)
		wB97XD	393.95 (1.5522)	31	HOMO→LUMO (50%), H-1→LUMO (45%)
<b>3A3</b>	401	CAM-B3LYP	386.45 (1.4923)	14	HOMO→LUMO (88%), H-1→LUMO (9%)
		wB97XD	383.73 (1.4702)	17	HOMO→LUMO (85%), H-1→LUMO (12%)
<b>3A4</b>	430	CAM-B3LYP	401.15 (1.6523)	29	HOMO→LUMO (59%), H-1→LUMO (35%)
		wB97XD	392.17 (1.7418)	38	H-1→LUMO (55%), HOMO→LUMO (38%)

<b>3A5</b>	451	CAM-B3LYP	419.56 (1.1600)	31	HOMO→LUMO (74%), H-2→LUMO (19%)
		wB97XD	399.43 (1.5936)	52	H-2→LUMO (45%), HOMO→LUMO (42%)
<b>3A6</b>	423	CAM-B3LYP	394.40 (1.6037)	29	HOMO→LUMO (49%), H-2→LUMO (43%)
		wB97XD	389.67 (1.6332)	33	H-2→LUMO (56%), HOMO→LUMO (33%)
<b>3A7</b>	454	CAM-B3LYP	434.58 (1.5677)	19	HOMO→LUMO (62%), HOMO→L+1 (27%), H-1→LUMO (9%)
		wB97XD	424.08 (1.5251)	30	HOMO→L+1 (66%), HOMO→LUMO (27%)

The respective fluorescence quantum yields for **3A1-7** are in the range of 13 to 62% (Table 5). For the tested compounds **3A1-7**, the attachment of a strong donor such as fluorene, carbazole, and bithiophene groups to the triazole ring gives rise to an increased quantum yield by up to 62% in the case of compound **3A7** with bithiophene group. The similar substituent effects of the donor group on quantum yield was observed in the case of terpyridine derivatives [30]. Among the specific compounds, compound **3A2**, which contains an electron-donating *p*-pentyloxyphenyl group, displays significantly reduced quantum yield ( $\Phi_{3A2} = 13\%$ ) compared to the compound with fluorene substituent **3A4** ( $\Phi_{3A4} = 52\%$ ). This probably indicates that the higher quantum efficiency of **3A4** is prominently affected by the larger  $\pi$ -conjugated system of fluorene group.

#### 2.4. Druglikeness analysis

Followed the trend of computational considerations which allow to predict ADME parameters (absorption, distribution, metabolism, and excretion), pharmacokinetic properties, druglike nature and medicinal chemistry friendliness, the calculations were done for **2A1-7** and **3A1-7** by using the web tool SwissADME [31]. The data obtained for target compounds, i.e. Log  $P_{o/w}$  (average values of all available predictions), topological polar surface area (TPSA), molar refractivity (AMR), number of H-bond acceptors (HBA) and donors (HBD) are presented in Table 8. Druglikeness for all compounds was checked by using the Lipiński (L) [32], Ghose (G) [33], Veber (V) [34], Egan (E) [35] and Muegge (M) [36] rules. The obtained result showed that in the case of aldehydes **2A1-7** only **2A5** containing carbazyl substituent does not meet the conditions of Ghose, Egan and Muegge rules, while there is no violation for the rest of compounds. The same investigation for malononitrile derivatives

**3A1-7** showed that the derivative of aldehyde **2A5**, i.e. **3A5** does not meet the same rules druglikeness rules, what is more, **3A4**, **3A6** and **3A7** also do not meet at least one of the rules.

**Table 8.** Druglikeness of molecules **2A1-7** and **3A1-7** based on Lipiński (L), Ghose (G), Veber (V), Egan (E) and Muegge (M) rules.

	L	G	V	E	M	MW [g/mol]	Log P <sub>o/w</sub>	TPSA [Å <sup>2</sup> ]	AMR	HBA	HBD
<b>2A1</b>						249.27	2.48	47.78	72.18	3	0
<b>2A2</b>						335.40	3.81	57.01	97.90	4	0
<b>2A3</b>						250.26	1.73	60.67	69.98	4	0
<b>2A4</b>						365.43	4.53	47.78	110.13	3	0
<b>2A5</b>						450.57	5.99	52.71	140.10	3	0
<b>2A6</b>						355.41	4.44	76.02	105.07	3	0
<b>2A7</b>						337.42	3.80	104.26	93.37	3	0
<b>3A1</b>						297.13	2.72	78.29	86.00	4	0
<b>3A2</b>						383.45	4.09	87.52	111.72	5	0
<b>3A3</b>						298.30	2.05	91.18	83.79	5	0
<b>3A4</b>						413.47	4.77	78.29	123.94	4	0
<b>3A5</b>						498.62	6.16	83.22	153.91	4	0
<b>3A6</b>						403.46	4.67	106.53	118.89	4	0
<b>3A7</b>						385.46	4.06	134.77	107.19	4	0

### 3. Conclusions

The target molecules **3A1-7** were obtained based on the presented efficient synthetic route with the yields in the range of 65-85%. The structures of the malononitrile derivatives have following electronic architecture Acceptor- $\pi$ -Acceptor-Acceptor/Donor (-CH<sub>2</sub>(CN)<sub>2</sub>-C<sub>6</sub>H<sub>4</sub>-/triazole/ substituent). The structures of compounds were confirmed by <sup>1</sup>H and <sup>13</sup>C NMR spectroscopy. Obtained target compounds are thermally stable, exhibit several absorption bands in the UV-Vis range. Furthermore, the molecules demonstrate strong blue-greenish photoluminescence in chloroform solution with the peaks located in the range of 400 - 455 nm. The nature of the optical properties was studied based on the results of DFT and TD-DFT results, it allowed to find the impact of the electron character of the substituent on the properties. The structural changes associated with position 4 of the triazole unit of **3A1-7** are quite pronounced and the impact of their electronic capacity is significant. In the case of the

bithiophene and carbazole motifs with strong electron-donating character were adopted to the triazole unit in **3A5** and **3A7**, respectively, the fluorescence peaks of presented compounds exhibited red shifts about 50 nm with relative to **3A3**, which possess strong electron-withdrawing pyridine unit. The respective fluorescence quantum yields for **3A1-7** are in the range of 13 to 62%. For the tested compounds **3A1-7**, the attachment of a strong donor such as fluorene, carbazole, and bithiophene groups to the triazole ring gives rise to an increased quantum yield by up to 62% in the case of compound **3A7** with bithiophene group. The druglikeness analysis based on the parameters of the well-known in literature Lipiński, Ghose, Veber, Egan and Muegge rules, showed that in the case of aldehydes **2A1-7** only **2A5** containing carbazyl substituent does not meet the conditions of Ghose, Egan and Muegge rules, while there is no violation for the rest of compounds. The same investigation for malononitrile derivatives **3A1-7** showed that **3A5** does not meet the same rules druglikeness rules as the aldehyde **2A5**, what is more, **3A4**, **3A6** and **3A7** also do not meet at least one of the rules. Obtained results and their deep analysis have emphasized the validity of synthesis of 4-(4-substituted-1*H*-1,2,3-triazol-1-yl)benzaldehyde as materials which exhibit interesting optical, photophysical and also biological properties, what can predestine them as materials dedicated to organic electronics and medicine. We believe that presented work will be an inspiration for other scientists.

### Acknowledgement

This work was supported by the Ministry of Science and Higher Education, Poland Diamantowy Grant number 0215/DIA/2015/44. D. Zych was financed by the National Science Centre of Poland ETIUDA 6 2018/28/T/ST5/00005.

Calculations have been carried out using resources provided by Wrocław Centre for Networking and Supercomputing (<http://wcss.pl>), grant No.18.

### 4. Experimental Section

**General Procedure for the synthesis of 2A1-2A7:** In a 100 mL round-bottom flask, 4-azidobenzaldehyde (0.080 g, 0.54 mmol), ethanol (21 mL) and water (9 mL) were placed. The mixture was saturated with argon for 15 minutes and then appropriate ethynyl aryl (0.66 mmol) (in the case of ethynyl derivatives protected by trimethylsilyl, the silyl group is removing *in situ* by using KF (0.051 g, 0.88 mmol)), sodium ascorbate (0.132 g, 0.66 mmol), CuSO<sub>4</sub>·5H<sub>2</sub>O (0.165 g, 0.66 mmol), and pyridine (0.5 mL) were added. The mixture was

stirred at room temperature for 48 h. Then, chloroform (30 mL) and 5% solution of ammonia (20 mL) were added, and the mixture was stirred for additional 30 min. The mixture was extracted with water (50 mL) and  $\text{CHCl}_3$  (2 x 50 mL). The combined organic layers were evaporated, and the crude product was dissolved in a small amount of  $\text{CHCl}_3$ , and the excess of hexane was added and put in the centrifuge tube into an ultrasonic bath for 5 min. The obtained precipitate was filtrated through the fritted funnel G3 and washed with water and diethyl ether.

**4-(4-Phenyl-1*H*-1,2,3-triazol-1-yl)benzaldehyde (2A1)** (105 mg, 78%) as solid  $^1\text{H}$  NMR (400 MHz,  $\text{CDCl}_3$ )  $\delta$  10.09 (s, 1H), 8.29 (s, 1H), 8.12 – 8.06 (m, 2H), 8.06 – 8.00 (m, 2H), 7.96 – 7.90 (m, 2H), 7.54 – 7.45 (m, 2H), 7.44 – 7.37 (m, 1H).  $^{13}\text{C}$  NMR (101 MHz,  $\text{CDCl}_3$ )  $\delta$  190.77, 149.13, 141.16, 136.15, 131.55, 129.90, 129.17, 128.94, 126.10, 120.56, 117.34.

**4-(4-(4-Pentyloxyphenyl)-1*H*-1,2,3-triazol-1-yl)benzaldehyde (2A2)** (139 mg, 77%) as solid  $^1\text{H}$  NMR (400 MHz,  $\text{CDCl}_3$ )  $\delta$  10.09 (s, 1H), 8.17 (s, 1H), 8.07 (d,  $J = 8.7$  Hz, 2H), 8.01 (d,  $J = 8.5$  Hz, 2H), 7.83 (d,  $J = 8.8$  Hz, 2H), 7.00 (d,  $J = 8.8$  Hz, 2H), 4.02 (t,  $J = 6.6$  Hz, 2H), 1.87 – 1.77 (m, 2H), 1.48 – 1.35 (m, 4H), 0.96 (t,  $J = 7.1$  Hz, 3H).  $^{13}\text{C}$  NMR (126 MHz,  $\text{CDCl}_3$ )  $\delta$  190.80, 159.79, 149.02, 141.17, 135.97, 131.49, 127.35, 122.23, 120.41, 116.40, 115.08, 68.25, 29.06, 28.32, 22.59, 14.15.

**4-(4-Pyrid-2-yl-1*H*-1,2,3-triazol-1-yl)benzaldehyde (2A3)** (85 mg, 63%) as solid  $^1\text{H}$  NMR (400 MHz,  $\text{CDCl}_3$ )  $\delta$  10.09 (s, 1H), 8.69 (s, 1H), 8.63 (d,  $J = 4.4$  Hz, 1H), 8.26 (d,  $J = 7.9$  Hz, 1H), 8.07 (q,  $J = 8.6$  Hz, 4H), 7.83 (td,  $J = 7.8, 1.7$  Hz, 1H), 7.32 – 7.26 (m, 1H).  $^{13}\text{C}$  NMR (126 MHz,  $\text{CDCl}_3$ )  $\delta$  190.77, 149.75, 149.62, 141.06, 137.25, 136.21, 131.57, 123.55, 120.72, 120.54, 119.89.

**4-(4-(9,9-Dimethylfluoren-2-yl)-1*H*-1,2,3-triazol-1-yl)benzaldehyde (2A4)** (128 mg, 65%) as solid  $^1\text{H}$  NMR (400 MHz,  $\text{CDCl}_3$ )  $\delta$  10.10 (s, 1H), 8.32 (s, 1H), 8.10 (d,  $J = 7.7$  Hz, 2H), 8.05 (d,  $J = 7.0$  Hz, 3H), 7.86 (d,  $J = 7.0$  Hz, 1H), 7.81 (d,  $J = 7.8$  Hz, 1H), 7.76 (d,  $J = 5.7$  Hz, 1H), 7.47 (d,  $J = 6.1$  Hz, 1H), 7.36 (d,  $J = 2.9$  Hz, 2H), 1.57 (s, 6H).  $^{13}\text{C}$  NMR (101 MHz,  $\text{CDCl}_3$ )  $\delta$  190.55, 154.76, 154.19, 149.65, 141.29, 140.17, 138.79, 136.30, 131.48, 128.86, 127.82, 127.27, 125.16, 122.83, 120.61, 120.49, 120.34, 117.21, 47.23, 27.31.

**4-(4-(9-Octyl-9H-carbazol-3-yl)-1H-1,2,3-triazol-1-yl)benzaldehyde (2A5)** (170 mg, 70%) as solid  $^1\text{H}$  NMR (400 MHz,  $\text{CDCl}_3$ )  $\delta$  10.08 (s, 1H), 8.66 (d,  $J = 1.4$  Hz, 1H), 8.32 (s, 1H), 8.16 (d,  $J = 7.7$  Hz, 1H), 8.10 – 8.02 (m, 4H), 8.00 (dd,  $J = 8.5, 1.6$  Hz, 1H), 7.53 – 7.46 (m, 2H), 7.43 (d,  $J = 8.1$  Hz, 1H), 7.28 (d,  $J = 7.2$  Hz, 1H), 4.32 (t,  $J = 7.2$  Hz, 2H), 1.97 – 1.82 (m, 2H), 1.44 – 1.31 (m, 4H), 1.31 – 1.19 (m, 6H), 0.87 (t,  $J = 6.8$  Hz, 3H).  $^{13}\text{C}$  NMR (101 MHz,  $\text{CDCl}_3$ )  $\delta$  190.79, 150.18, 141.26, 141.04, 140.79, 135.93, 131.46, 126.23, 123.91, 123.42, 122.92, 120.71, 120.65, 120.36, 119.36, 118.17, 116.36, 109.26, 109.10, 43.38, 31.92, 29.50, 29.31, 29.13, 27.45, 22.73, 14.19.

**4-(4-Dibenzo[b,d]thiophen-2-yl)-1H-1,2,3-triazol-1-yl)benzaldehyde (2A6)** (146 mg, 76%) as solid  $^1\text{H}$  NMR (400 MHz,  $\text{CDCl}_3$ )  $\delta$  10.09 (s, 1H), 8.77 (s, 1H), 8.39 (s, 1H), 8.30 – 8.23 (m, 1H), 8.12 – 8.02 (m, 4H), 7.95 (s, 2H), 7.91 – 7.83 (m, 1H), 7.55 – 7.44 (m, 2H).  $^{13}\text{C}$  NMR (126 MHz,  $\text{CDCl}_3$ )  $\delta$  190.79, 149.15, 141.11, 140.02, 139.99, 136.37, 136.16, 135.43, 131.57, 127.31, 126.33, 124.81, 124.60, 123.49, 123.08, 122.02, 120.55, 119.07, 117.33.

**4-(4-(2,2'-Bithiophenyl-5-yl)-1H-1,2,3-triazol-1-yl)benzaldehyde (2A7)** (109 mg, 60%) as solid  $^1\text{H}$  NMR (400 MHz,  $\text{CDCl}_3$ )  $\delta$  10.09 (s, 1H), 8.19 (s, 1H), 8.09 (d,  $J = 8.5$  Hz, 2H), 8.01 (d,  $J = 8.6$  Hz, 2H), 7.41 (d,  $J = 3.7$  Hz, 1H), 7.24 (d,  $J = 3.6$  Hz, 2H), 7.19 (d,  $J = 3.7$  Hz, 1H), 7.05 (dd,  $J = 5.0, 3.7$  Hz, 1H).

**General Procedure for the synthesis of 3A1-3A7:** In 25 mL Schlenk flask, **2A1-2A7** (0.2 mmol) and aluminium oxide (0.050 g) were placed, and the flask was three times evacuated and refilled with argon. During this time in the vial, dichloromethane (5 mL) was saturated with argon for 15 minutes, and then malononitrile (0.052 g, 0.8 mmol) was dissolved. The obtained mixture was added to the Schlenk flask by using a syringe and stirred for 24 h at room temperature. After that time, the crude product was purified by using the column chromatography ( $\text{SiO}_2/\text{DCM}:\text{EtOAc}:\text{Et}_2\text{O}$ ).

**2-[4-(4-Phenyl-1H-1,2,3-triazol-1-yl)benzylidene]malononitrile (3A1)** (50 mg, 81%) as solid  $^1\text{H}$  NMR (400 MHz,  $\text{CDCl}_3$ )  $\delta$  8.29 (s, 1H), 8.13 (d,  $J = 8.8$  Hz, 2H), 8.04 (d,  $J = 8.8$  Hz, 2H), 7.93 (d,  $J = 7.2$  Hz, 2H), 7.82 (s, 1H), 7.49 (t,  $J = 7.5$  Hz, 2H), 7.41 (t,  $J = 7.3$  Hz, 1H).

**2-[4-(4-(4-Pentyloxyphenyl)-1H-1,2,3-triazol-1-yl)benzylidene]malononitrile (3A2)**

(65 mg, 85 %) as solid  $^1\text{H}$  NMR (400 MHz,  $\text{CDCl}_3$ )  $\delta$  8.19 (s, 1H), 8.11 (d,  $J = 8.7$  Hz, 2H), 8.03 (d,  $J = 8.7$  Hz, 2H), 7.83 (d,  $J = 10.2$  Hz, 3H), 7.00 (d,  $J = 8.7$  Hz, 2H), 4.02 (t,  $J = 6.6$  Hz, 2H), 1.87 – 1.77 (m, 2H), 1.49 – 1.35 (m, 4H), 0.95 (t,  $J = 7.1$  Hz, 3H).

**2-[4-(4-Pyrid-2-yl-1H-1,2,3-triazol-1-yl)benzylidene]malononitrile (3A3)**

(47 mg, 79 %) as solid  $^1\text{H}$  NMR (400 MHz,  $\text{CDCl}_3$ )  $\delta$  8.72 (s, 1H), 8.64 (d,  $J = 4.1$  Hz, 1H), 8.27 (d,  $J = 7.9$  Hz, 1H), 8.13 (d,  $J = 8.8$  Hz, 2H), 8.06 (d,  $J = 8.8$  Hz, 2H), 7.88 – 7.80 (m, 2H), 7.34 – 7.29 (m, 1H).

**2-[4-(4-(9,9-Dimethylfluoren-2-yl)-1H-1,2,3-triazol-1-yl)benzylidene]malononitrile (3A4)**

(62 mg, 75 %) as solid  $^1\text{H}$  NMR (400 MHz,  $\text{CDCl}_3$ )  $\delta$  8.34 (s, 1H), 8.14 (d,  $J = 8.7$  Hz, 2H), 8.07 (d,  $J = 9.0$  Hz, 3H), 7.84 (q,  $J = 8.2$  Hz, 3H), 7.79 – 7.74 (m, 1H), 7.49 – 7.45 (m, 1H), 7.40 – 7.32 (m, 2H), 1.26 (s, 6H).

**2-[4-(4-(9-Octyl-9H-carbazol-3-yl)-1H-1,2,3-triazol-1-yl)benzylidene]malononitrile**

**(3A5)** (78 mg, 78 %) as solid  $^1\text{H}$  NMR (400 MHz,  $\text{CDCl}_3$ )  $\delta$  8.63 (d,  $J = 1.3$  Hz, 1H), 8.29 (s, 1H), 8.15 (d,  $J = 7.7$  Hz, 1H), 8.04 (q,  $J = 8.9$  Hz, 4H), 7.98 (dd,  $J = 8.5, 1.6$  Hz, 1H), 7.73 (s, 1H), 7.54 – 7.41 (m, 3H), 7.29 (d,  $J = 7.1$  Hz, 1H), 4.33 (t,  $J = 7.2$  Hz, 2H), 1.94 – 1.83 (m, 2H), 1.45 – 1.31 (m, 4H), 1.31 – 1.18 (m, 6H), 0.86 (t,  $J = 6.8$  Hz, 3H).  $^{13}\text{C}$  NMR (126 MHz,  $\text{CDCl}_3$ )  $\delta$  157.94, 150.38, 141.04, 140.88, 132.57, 130.53, 126.34, 123.91, 123.43, 122.88, 120.73, 120.50, 120.37, 119.44, 118.22, 115.96, 113.56, 112.54, 109.32, 109.16, 83.72, 43.42, 31.92, 29.51, 29.32, 29.15, 27.46, 22.74, 14.21.

**2-[4-(4-Dibenzo[b,d]thiophen-2-yl)-1H-1,2,3-triazol-1-yl)benzylidene]malononitrile (3A6)**

(66 mg, 82 %) as solid  $^1\text{H}$  NMR (400 MHz,  $\text{CDCl}_3$ )  $\delta$  8.78 (s, 1H), 8.40 (s, 1H), 8.28 (dd,  $J = 6.2, 3.0$  Hz, 1H), 8.11 (dd,  $J = 24.5, 8.8$  Hz, 4H), 7.96 (d,  $J = 1.0$  Hz, 2H), 7.89 (dd,  $J = 6.3, 2.8$  Hz, 1H), 7.83 (s, 1H), 7.53 – 7.50 (m, 2H).

**2-[4-(4-(2,2'-Bithiophenyl-5-yl)-1H-1,2,3-triazol-1-yl)benzylidene]malononitrile (3A7)**

(50 mg, 65 %) as solid  $^1\text{H}$  NMR (400 MHz,  $\text{CDCl}_3$ )  $\delta$  8.19 (s, 1H), 8.12 (d,  $J = 8.8$  Hz, 2H), 8.02 (d,  $J = 8.7$  Hz, 2H), 7.82 (s, 1H), 7.43 (d,  $J = 3.6$  Hz, 1H), 7.25 – 7.23 (m, 2H), 7.19 (d,  $J = 3.8$  Hz, 1H), 7.08 – 7.03 (m, 1H).

**References**

- [1] P. Wen, Z. Gao, R. Zhang, A. Li, F. Zhang, J. Li, J. Xie, Y. Wu, M. Wu, K. Guo, A- $\pi$ -D- $\pi$ -A carbazole derivatives with remarkable solvatochromism and mechanoresponsive luminescence turn-on, *J. Mater. Chem. C*. 5 (2017) 6136–6143. doi:10.1039/C7TC00559H.
- [2] S. Kotowicz, M. Siwy, M. Filapek, J.G. Malecki, K. Smolarek, J. Grzelak, S. Mackowski, A. Slodek, E. Schab-Balcerzak, New donor-acceptor-donor molecules based on quinoline acceptor unit with Schiff base bridge: synthesis and characterization, *J. Lumin.* 183 (2017) 458–469. doi:10.1016/J.JLUMIN.2016.11.058.
- [3] S. Sambathkumar, S. Priyadarshini, M. Fleisch, D.W. Bahnemann, G. Gnana Kumar, S. Senthilarasu, R. Renganathan, Design and synthesis of imidazole-triphenylamine based organic materials for dye sensitized solar cells, *Mater. Lett.* 242 (2019) 28–31. doi:10.1016/j.matlet.2019.01.091.
- [4] A. Slodek, D. Zych, S. Golba, S. Zimosz, P. Gnida, E. Schab-Balcerzak, Dyes based on the D/A-acetylene linker-phenothiazine system for developing efficient dye-sensitized solar cells, *J. Mater. Chem. C*. 7 (2019) 5830–5840. doi:10.1039/C9TC01727E.
- [5] M.J. Juríček, P.H.J. Kouwer, A.E. Rowan, Triazole: a unique building block for the construction of functional materials, *This J. Is Cite This Chem. Commun.* 47 (2011) 8740–8749. doi:10.1039/c1cc10685f.
- [6] G. de Miguel, M. Wielopolski, D.I. Schuster, M.A. Fazio, O.P. Lee, C.K. Haley, A.L. Ortiz, L. Echegoyen, T. Clark, D.M. Guldi, Triazole Bridges as Versatile Linkers in Electron Donor–Acceptor Conjugates, *J. Am. Chem. Soc.* 133 (2011) 13036–13054. doi:10.1021/ja202485s.
- [7] M.A. Fazio, O.P. Lee, D.I. Schuster, First Triazole-Linked Porphyrin–Fullerene Dyads, *Org. Lett.* 10 (2008) 4979–4982. doi:10.1021/ol802053k.
- [8] L. Yet, Five-Membered Ring Systems: With More than One N Atom, *Prog. Heterocycl. Chem.* 23 (2011) 231–266. doi:10.1016/B978-0-08-096805-6.00008-5.
- [9] D. Zych, A. Slodek, Pyrene derivatives with two types of substituents at positions 1, 3, 6, and 8 – fad or necessity?, *RSC Adv.* 9 (2019) 24015–24024. doi:10.1039/C9RA04503A.
- [10] D. Zych, A. Slodek, D. Matuszczyk, S. Golba, Comprehensive Study of Mononuclear Osmium Complexes with Various Pyrene Ligands, *Eur. J. Inorg. Chem.* 2018 (2018)

- 5117–5128. doi:10.1002/ejic.201801199.
- [11] L.L. Zanin, D.E.Q. Jimenez, L.P. Fonseca, A.L. Meleiro Porto, Knoevenagel Condensation Reactions of Cyano Malononitrile-Derivatives Under Microwave Radiation, *Curr. Org. Chem.* 22 (2018) 519–532. doi:10.2174/1385272822666180123145819.
- [12] Y. Chen, W. Shi, Y. Hui, X. Sun, L. Xu, L. Feng, Z. Xie, A new highly selective fluorescent turn-on chemosensor for cyanide anion, *Talanta*. 137 (2015) 38–42. doi:10.1016/J.TALANTA.2015.01.018.
- [13] Y. Li, J. Chen, T.-S. Chu, Sensing mechanism for a fluorescent off–on chemosensor for cyanide anion, *J. Lumin.* 179 (2016) 203–210. doi:10.1016/J.JLUMIN.2016.07.024.
- [14] Z. Xie, X. Kong, L. Feng, J. Ma, Y. Li, X. Wang, W. Bao, W. Shi, Y. Hui, A novel highly selective probe with both aggregation-induced emission enhancement and intramolecular charge transfer characteristics for CN<sup>−</sup> detection, *Sensors Actuators B Chem.* 257 (2018) 154–165. doi:10.1016/J.SNB.2017.10.167.
- [15] P.D. Jarowski, Y.-L. Wu, W.B. Schweizer, F. Diederich, 1,2,3-Triazoles as Conjugative  $\pi$ -Linkers in Push–Pull Chromophores: Importance of Substituent Positioning on Intramolecular Charge-Transfer, *Org. Lett.* 10 (2008) 3347–3350. doi:10.1021/ol801253z.
- [16] P. Luo, Y. Yu, D. Wu, X. Li, C. Dai, X. Chen, G. Li, Y. Wu, Simultaneous determination of cyanide and thiocyanate in swine plasma by high-performance liquid chromatography with fluorescence detection based on a novel D– $\pi$ –A carbazole-based turn-on fluorescence labeling reagent, *Anal. Methods*. 11 (2019) 2983–2990. doi:10.1039/C9AY00784A.
- [17] T. Gao, X. Cao, P. Ge, J. Dong, S. Yang, H. Xu, Y. Wu, F. Gao, W. Zeng, A self-assembled fluorescent organic nanoprobe and its application for sulfite detection in food samples and living systems, *Org. Biomol. Chem.* 15 (2017) 4375–4382. doi:10.1039/C7OB00580F.
- [18] G. Marianetti, M. Lessi, V. Barone, F. Bellina, A. Pucci, P. Minei, Solar collectors based on luminescent 2,5-diarylimidazoles, *Dye. Pigment.* 157 (2018) 334–341. doi:10.1016/J.DYEPIG.2018.04.062.
- [19] R. Domínguez, N.F. Montcada, P. de la Cruz, E. Palomares, F. Langa, Pyrrolo[3,2- *b*]pyrrole as the Central Core of the Electron Donor for Solution-Processed Organic Solar Cells, *Chempluschem*. 82 (2017) 1096–1104. doi:10.1002/cplu.201700158.

- [20] Z. Li, X. Li, H. Chen, C. He, L. Wang, Y. Yang, S. Wang, H. Guo, S.H. Liu, Multi-modulated photochromic behavior of a D-A type dithienylethene, *Dye. Pigment.* 162 (2019) 712–720. doi:10.1016/J.DYEPIG.2018.11.003.
- [21] Y.J. Chang, J.-L. Hsu, Y.-H. Li, S. Biring, T.-H. Yeh, J.-Y. Guo, S.-W. Liu, Carbazole-based small molecules for vacuum-deposited organic photovoltaic devices with open-circuit voltage exceeding 1 V, *Org. Electron.* 47 (2017) 162–173. doi:10.1016/J.ORGEL.2017.05.007.
- [22] D. Zych, A. Slodek, D. Zimny, S. Golba, K. Malarz, A. Mrozek-Wilczkiewicz, Influence of the substituent D/A at the 1,2,3-triazole ring on novel terpyridine derivatives: synthesis and properties, *RSC Adv.* 9 (2019) 16554–16564. doi:10.1039/C9RA02655J.
- [23] F. Texier-Boulet, A. Foucaud, Knoevenagel condensation catalysed by aluminium oxide., *Tetrahedron Lett.* 23 (1982) 4927–4928. doi:10.1016/S0040-4039(00)85749-4.
- [24] A.D. Becke, Density functional thermochemistry. III. The role of exact exchange, *J. Chem. Phys.* 98 (1993) 5648–5652. doi:10.1063/1.464913.
- [25] T. Yanai, D.P. Tew, N.C. Handy, A new hybrid exchange–correlation functional using the Coulomb-attenuating method (CAM-B3LYP), *Chem. Phys. Lett.* 393 (2004) 51–57. doi:10.1016/J.CPLETT.2004.06.011.
- [26] J.-D. Chai, M. Head-Gordon, Long-range corrected hybrid density functionals with damped atom–atom dispersion corrections, *Phys. Chem. Chem. Phys.* 10 (2008) 6615. doi:10.1039/b810189b.
- [27] Y. Zhao, D.G. Truhlar, The M06 suite of density functionals for main group thermochemistry, thermochemical kinetics, noncovalent interactions, excited states, and transition elements: two new functionals and systematic testing of four M06-class functionals and 12 other functionals, *Theor. Chem. Acc.* 120 (2008) 215–241. doi:10.1007/s00214-007-0310-x.
- [28] Frisch, G. Trucks, H. Schlegel, G. Scuseria, M. Robb, J. Cheeseman, G. Scalmani, V. Barone, B. Mennucci, G. Petersson, H. Nakatsuji, M. Caricato, X. Li, H. Hratchian, A. Izmaylov, J. Bloino, G. Zheng, J. Sonnenberg, M. Hada, M. Ehara, K. Toyota, R. Fukuda, J. Hasegawa, M. Ishida, T. Nakajima, Y. Honda, O. Kitao, H. Nakai, T. Vreven, J. Montgomery, J. Peralta, F. Ogliaro, M. Bearpark, J. Heyd, E. Brothers, K. Kudin, V. Staroverov, R. Kobayashi, J. Normand, K. Raghavachari, A. Rendell, J. Burant, S. Iyengar, J. Tomasi, M. Cossi, N. Rega, J. Millam, M. Klene, J. Knox, J. Cross, V. Bakken, C. Adamo, J. Jaramillo, R. Gomperts, R. Stratmann, O. Yazyev, A.

- Austin, R. Cammi, C. Pomelli, J. Ochterski, R. Martin, K. Morokuma, V. Zakrzewski, G. Voth, P. Salvador, J. Dannenberg, S. Dapprich, A. Daniels, Farkas, J. Foresman, J. Ortiz, J. Cioslowski, D. Fox, Gaussian 09, Revision B.01, Gaussian 09, Revis. B.01, Gaussian, Inc., Wallingford CT. (2009).
- [29] G. Scalmani, M.J. Frisch, Continuous surface charge polarizable continuum models of solvation. I. General formalism, *J. Chem. Phys.* 132 (2010) 114110. doi:10.1063/1.3359469.
- [30] D. Zych, A. Słodek, S. Krompiec, K. Malarz, A. Mrozek-Wilczkiewicz, R. Musiol, 4'-Phenyl-2,2':6',2''-terpyridine Derivatives Containing 1-Substituted-2,3-Triazole Ring: Synthesis, Characterization and Anticancer Activity, *ChemistrySelect*. 3 (2018) 7009–7017. doi:10.1002/slct.201801204.
- [31] A. Daina, O. Michielin, V. Zoete, SwissADME: a free web tool to evaluate pharmacokinetics, drug-likeness and medicinal chemistry friendliness of small molecules, *Sci. Rep.* 7 (2017) 42717. doi:10.1038/srep42717.
- [32] C.A. Lipinski, F. Lombardo, B.W. Dominy, P.J. Feeney, Experimental and computational approaches to estimate solubility and permeability in drug discovery and development settings., *Adv. Drug Deliv. Rev.* 46 (2001) 3–26. <http://www.ncbi.nlm.nih.gov/pubmed/11259830> (accessed October 9, 2019).
- [33] A.K. Ghose, V.N. Viswanadhan, J.J. Wendoloski, A knowledge-based approach in designing combinatorial or medicinal chemistry libraries for drug discovery. 1. A qualitative and quantitative characterization of known drug databases., *J. Comb. Chem.* 1 (1999) 55–68. <http://www.ncbi.nlm.nih.gov/pubmed/10746014> (accessed October 9, 2019).
- [34] D.F. Veber, S.R. Johnson, H.-Y. Cheng, B.R. Smith, K.W. Ward, K.D. Kopple, Molecular Properties That Influence the Oral Bioavailability of Drug Candidates, *J. Med. Chem.* 45 (2002) 2615–2623. doi:10.1021/jm020017n.
- [35] W.J. Egan, K.M. Merz., J.J. Baldwin, Prediction of Drug Absorption Using Multivariate Statistics, *J. Med. Chem.* 43 (2000) 3867–3877. doi:10.1021/jm000292e.
- [36] I. Muegge, S.L. Heald, D. Brittelli, Simple Selection Criteria for Drug-like Chemical Matter, *J. Med. Chem.* 44 (2001) 1841–1846. doi:10.1021/jm015507e.

**Author Contribution Statement**

Dawid Zych: Conceptualization; Data collection; Funding acquisition; Investigation; Methodology; Writing - original draft, review & editing.

Aneta Slodek: Data collection; Investigation; Methodology; Writing - original draft, review & editing.

Journal Pre-proof

**Declaration of interests**

The authors declare that they have no known competing financial interests or personal relationships that could have appeared to influence the work reported in this paper.

The authors declare the following financial interests/personal relationships which may be considered as potential competing interests:

Journal Pre-proof